Reac Kinet Mech Cat (2015) 116:467–478
DOI 10.1007/s11144-015-0912-6

A mechanistic study of the sulfur tolerance of Cu–V mixed oxides in toluene catalytic combustion

Xinhua Zhang[1] · Zhiying Pei[1] · Tingting Wu[1] · Hanfeng Lu[2] · Haifeng Huang[1]

Received: 7 May 2015 / Accepted: 22 July 2015 / Published online: 30 July 2015

Abstract A number of copper and vanadium mixed oxides were synthesized using the sol–gel method and their sulfur tolerance was studied in toluene combustion (used as a model reaction) in the presence of SO_2. The results revealed that the activity and thio-tolerance ability of Cu–V mixed oxides were significantly related to their compositions. The Cu_1V_6 sample (1 and 6 are the atomic ratio of copper and vanadium in the mixed oxide) showed the best activity and thio-tolerance ability as compared with the other samples used in the study. The high performance of Cu_1V_6 sample could be related to the formation of CuV_2O_6 that restrained the formation of sulfate species, high specific surface area and good reducibility as characterized by XRD, FT-IR, N_2-physical adsorption/desorption and H_2-TPR.

Keywords Copper oxide · Vanadium oxide · Toluene · Catalytic combustion · Thio-tolerance · SO_2

Introduction

Catalytic oxidation is identified as the most efficient, energy-saving and environmentally friendly technique to abate volatile organic compound (VOC) emissions among many end-of-pipe abatement techniques [1, 2]. However, the gases emitted from some industries (e.g., soap factories, refineries, wastewater treatment plants, geothermal power plants, meat processing plants and some chemical plants) contain a certain amount of sulfur-containing compounds [3]. These compounds in the feed

✉ Haifeng Huang
hhf66@zjut.edu.cn

[1] College of Biological and Environmental Technology, Zhejiang University of Technology, Hangzhou 310032, People's Republic of China

[2] College of Chemical Engineering, Zhejiang University of Technology, Hangzhou 310032, People's Republic of China

gas can be easily transformed into SO_2 under the conditions of catalytic combustion [4], which usually results in catalyst poisoning [1, 5].

Generally, supported noble metal catalysts show relatively high activity in the catalytic combustion of VOCs at low temperatures [6]. However, these catalysts are easily poisoned in the presence of SO_2 due to the formation of stable sulfate species on their surfaces [6–8]. Therefore, many efforts have been made to modify the formulations of noble catalysts to improve their thio-tolerance abilities. For example, using Pt–Pd [6, 9], Ru–Pt [10], Rh–Pt [10, 11], Ir–Pt [6], Pd–Rh [11], Pd–Au [12] bimetal materials, or supporting noble metals on Al_2O_3 [8, 9, 13–18], ZrO_2 [6, 10, 15], SiO_2 [12, 13, 15, 19], CeO_2 [13, 18], TiO_2 [15, 19], SBA-15 [20], Co_3O_4 [21, 22] and even using the mixed oxide supports [7, 11, 14, 23, 24]. Although these modifications have some positive effects on the thio-tolerance ability of noble metal catalysts, the results are still not satisfactory.

Although metal oxide catalysts are less active than supported noble metal catalysts in VOC combustion at low temperatures, they work better in the presence of SO_2 [4, 25, 26]. Some mixed metal oxide catalysts such as SnO_2–Cr_2O_3 [27], SnO_2–In_2O_3 [25], $LaMn_{1-x}Mg_xO_3.yMgO$ [28] and $LaCr_{0.5-x}Mn_xMg_{0.5}O_3.yMgO$ [29, 30] are reported to have good thio-tolerance abilities in hydrocarbon catalytic combustion in the presence of SO_2. Copper-based oxide catalyst usually shows high activity in VOC combustion [31–33]. However, CuO easily reacts with SO_2 to form sulfate species on the catalyst surface and in turn the copper sulfate occupies the catalytic reactive sites [34]. The problem of thio-tolerance ability of the copper-based catalyst in sulfur-containing VOC combustion still needs to be resolved. Vanadium-based catalysts usually show good thermal stability and have been broadly used in industrial sulfuric production process [35]. Therefore, it is assumed that the thio-tolerance ability of Cu–V mixed oxides would be superior to the single component ones in VOC combustion in the presence of SO_2.

In the present work, a series of copper-vanadium mixed oxide catalysts were prepared by sol–gel method and used in toluene combustion in the presence of SO_2. Our aim is to study the relationship between catalytic activity, thio-tolerance ability and textural properties of the prepared catalysts.

Catalysts preparation

Cu_xV_y mixed oxide catalysts (x and y represent the atomic ratio of copper and vanadium in the samples) were prepared by sol–gel method using $Cu(NO_3)_2{\cdot}3H_2O$, NH_4VO_3 and citric acid as precursors. In a typical synthesis process, $Cu(NO_3)_2{\cdot}3H_2O$ and NH_4VO_3 were dissolved in deionized water to form 1.0 M homogenous solution. 1.0 M citric acid was added slowly to the above mentioned solution with continuous stirring at 70 °C in a water bath until a sticky gel is formed. The gel was dried at 110 °C for 10 h, and then calcined in air at 450 °C for 3 h to remove the organic compounds. These samples were denoted as Cu_xV_y (where x: y = 1:6, 1:1, and 6:1). For comparison, CuO_x and VO_x were also prepared by using the same method as mentioned above.

Catalyst characterization

XRD analysis

Powder X-ray diffraction patterns (XRD) of samples were recorded on an X'Pert Pro powder diffractometer using Cu K_α radiation (40 kV and 50 mA) and nickel filter. The diffractograms were recorded within 2θ range of 20°–80° with a 2θ step speed of 4°/min, and jade 5.0 software was used to analyze the phase compositions of as-prepared samples.

N_2-physical adsorption and desorption

N_2-physical adsorption/desorption isotherms were measured at −196 °C on Micromeritics ASAP 2020 C instrument. The samples were outgassed at 250 °C for 3 h before measurement, and the specific surface area were calculated using two parameters BET equation.

H_2-TPR analysis

H_2 programmed-temperature reduction (H_2-TPR) was investigated on FINE SORB-3010 instrument by heating 100 mg samples in H_2/Ar mixture gas (H_2 8 sccm and Ar 32 sccm) with the heating rate of 10 °C/min from 50 °C to 900 °C. The hydrogen consumption was monitored by thermo-conductivity detector (TCD). All the samples were heated in Ar atmosphere at 400 °C for 2 h and then cooled down to 50 °C in the same atmosphere before measurement.

Catalytic activity test

Catalytic oxidation experiments were performed in fixed bed quartz glass tubular reactor (6 mm inner diameter) at ambient pressure. 0.15 g catalyst was placed in the middle of the reactor and diluted with 1.5 g quartz sand. Each end of the reactor bed was packed with quartz wool to prevent the catalyst from draining off. Simulated toluene effluent was generated by bubbling the formulated air through the saturator in ice bath, and air as balance gas to give the desirable gas hourly space velocity (GHSV) in the catalytic reactor bed. The feed toluene concentration was kept at constant at 8000 ppm with a corresponding total GHSV of 50,000 mL g^{-1} h^{-1}. SO_2 was added in the feed gas to investigate the catalysts thio-tolerance ability. All gas flow was controlled by a mass flow controller (MFC, Beijing Seven-star Electronics Co., Ltd). The off-gas was analyzed by an online gas chromatograph (Agilent 6890 N) equipped with a FID detector. Toluene conversion without catalyst was below 3 percent in all experiments.

Results and discussion

Catalytic activity results

Light-off curves of Cu–V mixed oxides in toluene combustion in the absence of SO_2 are shown in Fig. 1. The Cu_1V_6 sample showed the highest activity among all investigated samples, where T_{50} (temperature with 50 % toluene conversion) is only 305 °C, about 100 °C lower than that of VO_x sample (T_{50} is 409 °C). Based on T_{50}, toluene combustion activity of the tested samples was $Cu_1V_6 > Cu_6V_1 > Cu_1V_1 > CuO_x > VO_x$. The main products of toluene combustion were CO_2 and H_2O, and apart from small amounts of CO detected in low-temperature range, no other secondary by-products were detected. At 400 °C, the selectivity to CO_2 was 100 % for all tested samples. Bulk copper oxide catalyst showed relatively high activity in toluene combustion, which is consistent with the reported literatures [36–38].

Toluene catalytic combustion is a common model reaction in VOC oxidation. Based on transition metal oxide catalysts, our work is compared with those recently reported in the literatures, and the results are listed in Table 1.

It is very difficult to compare the results of this work with those reported in the literature since the activity of the tested catalysts significantly depends on the operation conditions used. It is generally accepted that the light-off temperature (T_{50}) increases with the increase of feed concentration and GHSV. As listed in Table 1, the Cu_1V_6 sample tested at high toluene feed concentration and GHSV shows comparable activity as compared with the catalysts tested at relatively low feed concentration and GHSV, and even superior to the CuO/γ-Al_2O_3 tested under lower toluene feed concentration and GHSV.

The activity of Cu_xV_y samples in toluene catalytic combustion at 350 °C was also investigated in the presence of SO_2 and the results are shown in Fig. 2. All samples

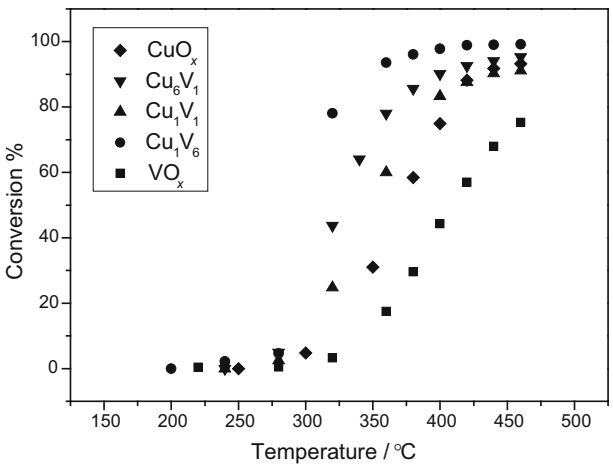

Fig. 1 Light-off curves of Cu_xV_y samples in toluene combustion in the absence of SO_2. Gas composition: 8000 ppm toluene, air balance; GHSV = 50,000 mL g_{cat}^{-1} h^{-1}

Table 1 Toluene catalytic combustion activity reported in literatures with transition metal oxides

Refs.	Catalyst(s) used	Toluene content/ppm	GHSV	T_{50}/ °C
[39]	Au–Co/SBA-15	1100	50,000 h^{-1}	287
[40]	CuO	226	60,000 h^{-1}	272
	5.0 % Au/CuO	226	60,000 h^{-1}	264
[41]	CuO/γ-Al_2O_3	1000	21,000·h^{-1}	313
[42]	9.5 %CuO/HCLT	1000	15,000 h^{-1}	330
[43]	Copper Vanadate	800	50,000 mL g^{-1} h^{-1}	265
This work	Cu_1V_6	8000	50,000 mL g^{-1} h^{-1}	305

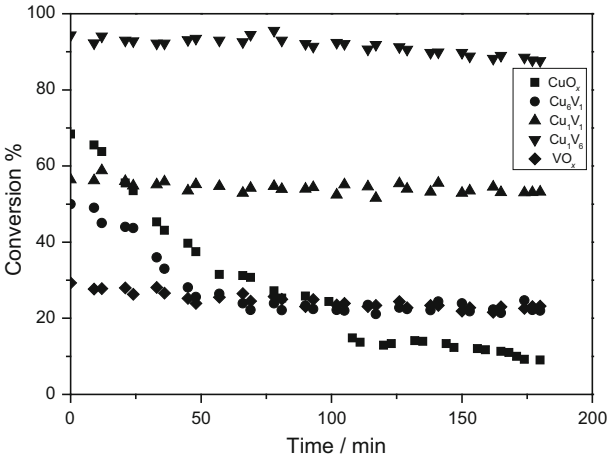

Fig. 2 Toluene conversion with time on stream in the presence of SO_2 at 350 °C. Test conditions: 8000 ppm toluene, 30 ppm SO_2, air balance, GHSV = 50,000 mL g_{cat}^{-1} h^{-1}

showed different levels of deactivation, depending on their compositions. Cu_1V_6 showed higher activity and stability as compared with the other tested samples. It is noteworthy that the CuO_x sample, which showed high toluene conversion in the absence of SO_2, undergoing severe deactivation in the presence of SO_2, the activity is lost about 68 % in a 180-min test. Similar results were also reported by Zhang et al. [34]. Using FT-IR and XRD characterizations, they found that the surface of active CuO_x is transformed into inactive $CuSO_4$. This might be the same reason for CuO_x deactivation observed in our work.

Since Cu_1V_6 sample shows good toluene combustion activity in the presence of SO_2. To further investigate the thermo-stability of Cu_1V_6, this sample was calcined at different temperatures in air and tested in toluene combustion in the presence of SO_2. The results are shown in Fig. 3.

As shown in Fig. 3, all the samples showed good thio-tolerance ability in the presence of SO_2, however, their toluene combustion activities were far away from

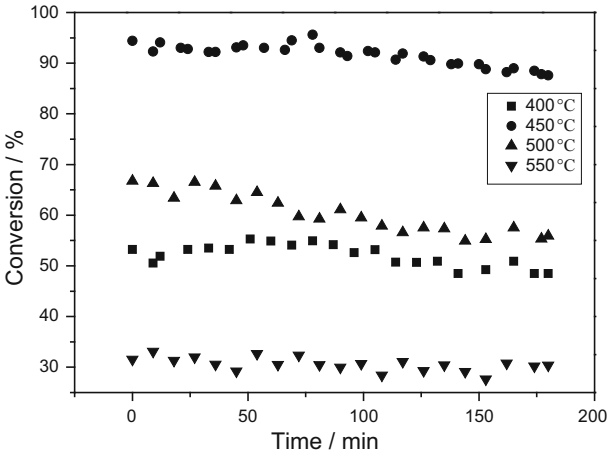

Fig. 3 Toluene conversion over Cu_1V_6 calcined at different temperatures. Testing conditions: 8000 ppm toluene, 30 ppm SO_2, air balance, GHSV = 50,000 mL g_{cat}^{-1} h^{-1}, 350 °C

identical. The sample calcined at 450 °C showed the best activity as compared with those calcined at the other temperatures.

XRD results

XRD patterns of the prepared copper-vanadium mixed oxides are shown in Fig. 4. The main diffractions of the pure copper oxide were indexed to tenorite phase (JCPDS PDF 48–1548). The VO_x sample showed the diffraction characteristics of V_2O_5 phase (JCPDS PDF 77–2418). Both $Cu_3V_2O_8$ phase (JCPDS PDF 74–1401)

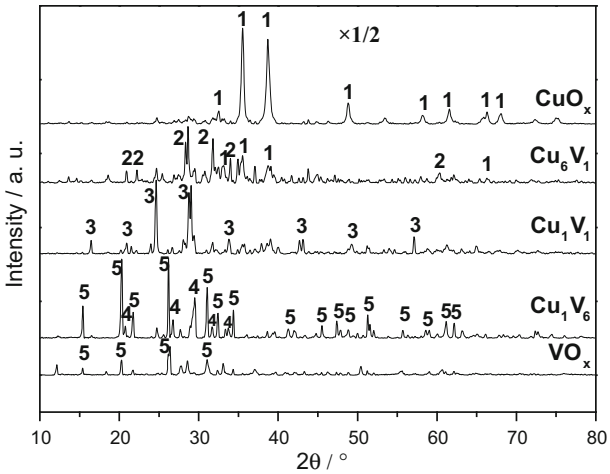

Fig. 4 XRD patterns of the samples (*1*: CuO, *2*: $Cu_3V_2O_8$, *3*: $Cu_2V_2O_7$, *4*: CuV_2O_6, *5*: V_2O_5)

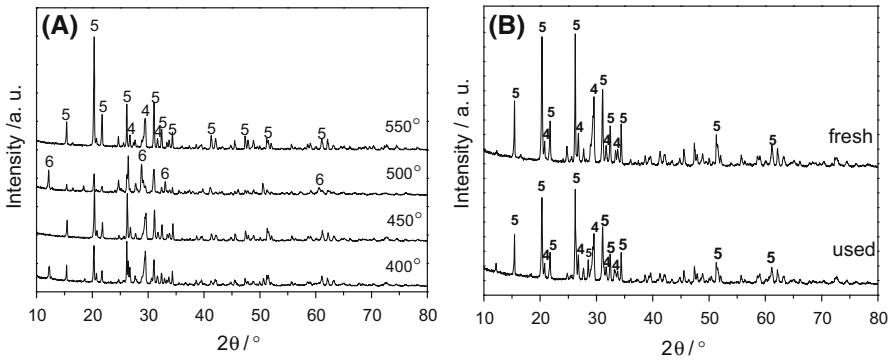

Fig. 5 XRD patterns of Cu_1V_6 sample calcined at different temperatures (**a**) and the used Cu_1V_6 sample (in toluene combustion in the presence of SO_2 at 350 °C) (**b**). (*4*-CuV_2O_6, *5*-V_2O_5 and *6*-$Cu_{0.261}$ [V_2O_5])

and tenorite phase were observed in Cu_6V_1 sample. However, the Cu_1V_1 sample showed the main phase of $Cu_2V_2O_7$ (JCPDS PDF 73–1032). The Cu_1V_6 sample with high content of vanadium showed the main diffractions of CuV_2O_6 phase (JCPDS PDF 74–2117) and V_2O_5 phase. No characterization diffraction peaks corresponding to the tenorite phase could be observed, and this would be benefit for the thio-tolerance ability of the sample.

The XRD patterns of Cu_1V_6 sample calcined at different temperatures, as well as the sample (calcined at 450 °C) after used in toluene combustion in the presence of SO_2 were also investigated. The results are shown in Fig. 5. The V_2O_5 and CuV_2O_6 phases were well retained on all samples except the sample calcined at 500 °C, which showed main phases of V_2O_5 and $Cu_{0.261}[V_2O_5]$ (ICSD# 79-0796). The phase compositions and corresponding crystal sizes are listed in Table 2. Compared with the sample calcined at 400 °C, the crystal size of V_2O_5 decreased at high calcination temperature. Interestingly, the sample calcined at 450 °C showed the smaller crystal sizes of V_2O_5 and CuV_2O_6 as compared with the other calcination temperature, which is consistent with the results of the biggest specific surface area observed in BET test (shown in Fig. 6). The phase compositions of Cu_1V_6 (calcined at 450 °C) after used in toluene combustion in the presence of SO_2 were well retained. No characteristic peaks corresponding to sulfates were observed, indicating there are no sulfates formed on the sample, or the amounts of sulfates are too little to be detected by the conventional XRD methods.

N_2-physical adsorption/desorption results

N_2-physical adsorption/desorption was carried out to investigate the specific surface area of Cu–V mixed oxides and the results are shown in Fig. 6. All specific surface areas of Cu–V mixed oxides was larger than those of CuO and V_2O_5. Cu_1V_6 sample showed the largest specific surface area as compared with the other investigated samples, which could be beneficial for the adsorption of reactant molecules on it.

Table 2 Phase compositions and corresponding crystal sizes of Cu_1V_6 sample calcined at different temperatures and the used Cu_1V_6 sample (in toluene combustion in the presence of SO_2 at 350 °C)

Calcination temperature/ °C	Phase compositions	Crystal sizes/nm
400	V_2O_5	68.6[a]
	CuV_2O_6	21.1[b]
450 (fresh)	V_2O_5	55.8
	CuV_2O_6	21.2
450 (used)	V_2O_5	49.2
	CuV_2O_6	34.0
500	V_2O_5	64.7
	$Cu_{0.261}[V_2O_5]$	67.3[c]
550	V_2O_5	64.5
	CuV_2O_6	24.8

[a, b, c] Calculated from the (0 0 1), (2 0 1) and (−1 1 1) diffractions of V_2O_5, CuV_2O_6 and $Cu_{0.261}[V_2O_5]$, respectively

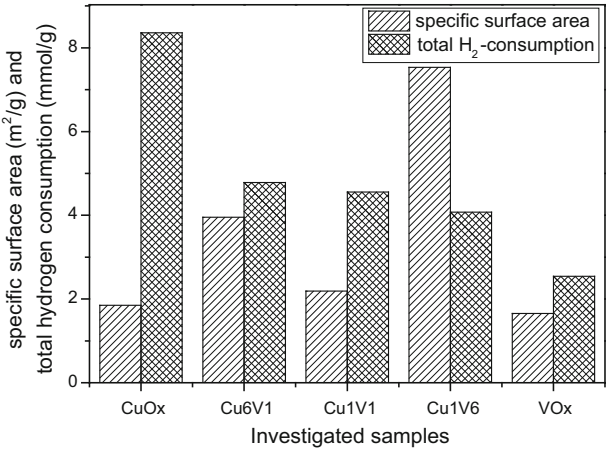

Fig. 6 Specific surface area and total hydrogen consumption of the investigated samples

H_2-TPR results

H_2-TPR measurements of Cu–V mixed oxides were carried out and the results are shown in Figs. 6 and 7. The CuO_x sample showed one reduction peak at ~234.3 °C corresponding to the reduction of bulk CuO [31, 44]. Vanadium is usually reduced at 600–700 °C [45], the two reduction peaks of VO_x sample at 626.6 °C and 684.3 °C could be attributed to the reduction of bulk V_2O_5. The first reduction peak was related to the reduction of V_2O_5 to V_6O_{13}, and the latter was related to the reduction of V_6O_{13} to V_2O_4 [46]. As compared with the VO_x sample, the reduction peaks of Cu–V mixed oxides were shifted to the low temperature range, indicating

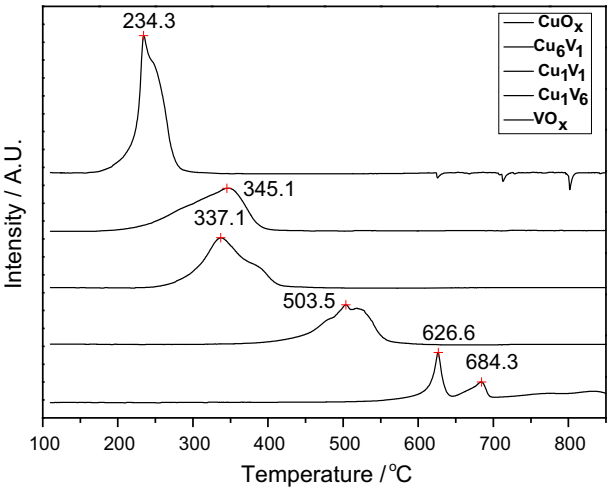

Fig. 7 H_2-TPR profiles of Cu-V mixed oxides

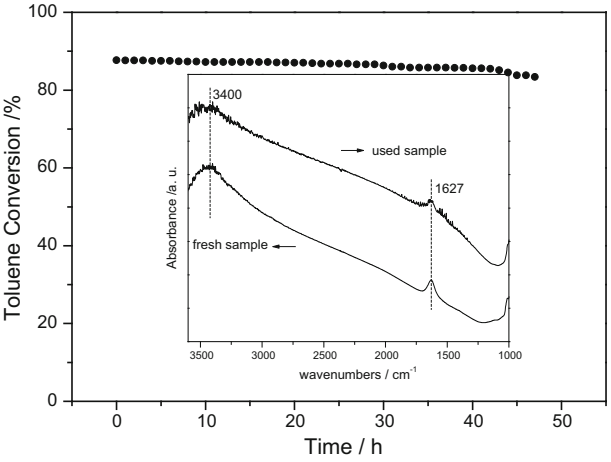

Fig. 8 Durability test of Cu_1V_6 sample (Test conditions: 8000 ppm toluene, 30 ppm SO_2, air balance, GHSV = 50,000 mL g_{cat}^{-1} h^{-1}, 350 °C. The inset is the FT-IR spectra of the fresh and the used samples)

the reducibility of Cu–V mixed oxides is superior to that of VO_x. As can be seen in Fig. 6, the total hydrogen consumption increases with the increase of copper content in the mixed oxides, indicating the good reducibility of Cu than that of V. However, the activity of toluene combustion and thio-resistance ability do not correspond to the materials with the best reducibility properties (as shown in Figs. 1 and 2). Thus, the other properties would determine the activity and thio-resistance ability of this sample, due to the phase compositions and the specific surface areas.

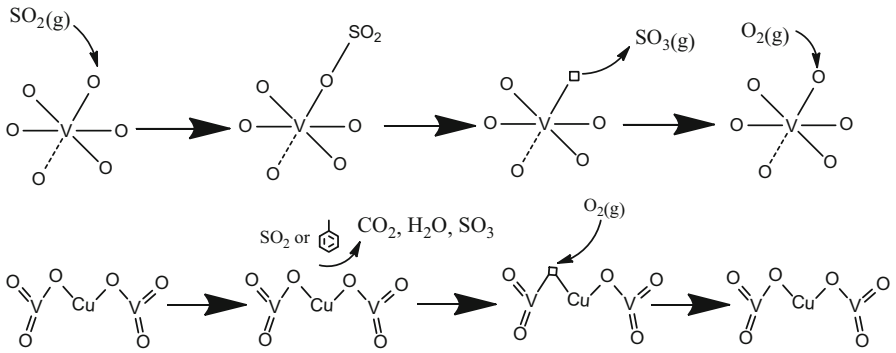

Fig. 9 The pathway of toluene catalytic combustion in the presence of SO_2 over Cu_1V_6 sample (*square*: oxygen vacancies)

Durability test of Cu_1V_6 sample

The durability of Cu_1V_6 sample in toluene combustion in the presence of SO_2 was investigated and the result is shown in Fig. 8. The sample showed a slight deactivation in a 48-h continuous test. The conversion of toluene was maintained above 83 %. No significant difference was observed in the FT-IR spectra of the fresh and the used samples (inset). The bands in 1627 and 3400 cm^{-1} could be attributed to the deformation vibration and stretching vibration of water molecule in the sample, respectively. Usually, the strong characteristic absorption peak of sulfate ion is located in range of 1210–1040 cm^{-1}, this band was not observed in the infrared spectrogram of the used Cu_1V_6 sample, indicating no sulfate formed on the surface of it. The slightly deactivation of Cu_1V_6 could be due to the decrease of the specific surface area (reduced about 3 % after 48 h of test).

Discussion

Copper oxide showed good activity in toluene total oxidation. However, it was severely poisoned in the presence of SO_2. Vanadia is a strong acidic transition metal oxide and always showed good tolerance in sulfur containing atmosphere. Unfortunately, vanadium oxide alone showed low activity during toluene combustion as shown in Fig. 1. Cu–V mixed oxides prepared by the sol–gel method showed good activity in toluene combustion in the presence of SO_2 as compared with that of VO_x. However, their stability is significantly different, depending on their compositions. The Cu_1V_6 sample showed the highest activity and thio-tolerance ability in toluene combustion in the presence of SO_2. XRD characterization revealed that this sample is composed of two main phases, i.e., V_2O_5 and CuV_2O_6, while Cu_1V_1 showed only a $Cu_2V_2O_7$ phase, and Cu_6V_1 sample showed mixed phases of CuO and $Cu_3V_2O_8$. The results are mainly consistent with the phase diagram of CuO–V_2O_5 system, as reported by Fleury [47]. The crystal structure of CuV_2O_6 consists of distorted octahedral VO_6, while $Cu_2V_2O_7$ consists of two V–O tetrahedral structures linked by two Cu^{2+} ions,

and $Cu_3V_2O_8$ consists of oxygen tetrahedrally coordinated to V^{5+} ion and octahedrally coordinated to Cu^{2+} ion. It is reported that the tetrahedrally coordinated vanadium species are inactive in SO_2 oxidation [35]. Thus, the Cu_1V_1 sample showed good thio-tolerance in toluene combustion in the presence of SO_2. The deactivation of Cu_6V_1 and CuO_x samples could be related to the existence of copper oxide phase, which can react with SO_2, forming stable sulfates on the surface of the catalyst, hence, occupied the active sites for toluene oxidation [34]. For Cu_1V_6 and VO_x, the two samples both have V_2O_5 phase in them and showed good stability in toluene combustion in the presence of SO_2, although they show different activity in toluene conversion. It is generally accepted that the uptake of SO_2 on the surface of bulk V_2O_5 is limited since the quantity of basic sites for the adsorption of SO_2 is negligible [48]. Thus, the small amount of adsorbed SO_2 may coordinate onto the V–O bond of either isolated or polymerized surface vanadium species, and resulting the $(V^{5+})\cdot SO_2$-ads state, then, followed by the cleavage of the V^{5+}–O–SO_2 and formation of SO_3(g). The reduced vanadia sites are re-oxidized by dissociatively absorbed oxygen and regenerating the active (V^{5+}) sites. For Cu_1V_6 sample, the low concentration of SO_2 selectively adsorbed on the surface of CuV_2O_6 sites with low acidity rather than adsorbed on the surface of V_2O_5 with strong acidity. The adsorbed SO_2 may be oxidized by oxygen from the Cu–O–V sites accompanied by the reduction of Cu^{2+} to Cu^{+} [49]. The sulfate formation on the CuV_2O_6 could be restrained as indicated by XRD and FT-IR characterizations (Figs. 5 and 8), thus the Cu_1V_6 sample showed good thio-tolerance as compared with those Copper-rich samples. Thus, based on the above discussions, a plausible reaction pathway can be proposed for toluene combustion over Cu_1V_6 sample in the presence of SO_2, as shown in Fig. 9.

Conclusions

Copper and vanadium mixed oxides were prepared by the sol–gel method to investigate their performances in the oxidation of toluene in the absence and presence of SO_2. The results revealed that the catalytic toluene combustion activity and the thio-tolerance ability of the prepared samples were significantly dependent on their compositions. Cu–V mixed oxides showed better performance as compared with CuO_x and VO_x samples. Cu_1V_6 sample was found to be the best catalyst among all investigated samples. The biggest specific surface area and the formation of CuV_2O_6 phase, as well as the increased reducibility as the introduction of copper in Cu_1V_6 sample will account for the good toluene combustion activity in the presence of SO_2. Therefore, Cu_1V_6 sample showed good durability during long term exposure to SO_2.

Acknowledgments The authors thank the financial support of Open-end Foundation of environmental science and engineering top priority discipline of Zhejiang Province (No. G2853105014).

References

1. Ojala S et al (2011) Top Catal 54:1224–1256

2. Li WB, Gong H (2010) Acta Phys-Chim Sin 26:885–894
3. Parus WJ, Paterkowski W (2009) Pol J Chem Tech 11:30–37
4. Ordonez S, Paredes JR, Diez FV (2008) Appl Catal A 341:174–180
5. Huang H et al (2010) Reac Kinet Mech Cat 101:417–427
6. Ohtsuka H (2011) Catal Let 141:413–419
7. Zi X et al (2011) Catal Today 175:223–230
8. Gelin P et al (2003) Catal Today 83:45–57
9. Corro G, Cano C, Fierro JLG (2010) J Mol Catal A 315:35–42
10. Ohtsuka H (2013) Catal Let 143:1043–1050
11. Cimino S et al (2010) Catal Today 154:283–292
12. Venezia AM et al (2007) J Catal 251:94–102
13. Bounechada D et al (2013) Phys Chem 15:8648–8661
14. Colussi S et al (2010) Catal Today 55:59–65
15. Escandon LS et al (2008) J Hazard Mater 153:742–750
16. Arosio F et al (2006) Catal Today 117:569–576
17. Hurtado P et al (2004) Appl Catal B 47:85–93
18. Escandon LS et al (2003) Catal Today 78:191–196
19. Di Carlo G et al (2010) Chem Commun 46:6317–6319
20. Liotta LF et al (2012) Top Catal 55:782–791
21. Liotta LF et al (2007) Appl Catal B 75:182–188
22. Liotta LF et al (2007) Top Catal 42:425–428
23. Arosio F et al (2008) Appl Catal B 80:335–342
24. Xue B et al (2007) Gong Cuihua 15:19–24
25. Li J et al (2006) Environ Sci Tech 40:6455–6459
26. Decker SP et al (2002) Environ Sci Tech 36:762–768
27. Zhou C et al (2003) Wuli Huaxue Xuebao 19:246–250
28. Rosso I et al (2001) Appl Catal B 34:29–41
29. Rosso I et al (2003) Appl Catal B 40:195–205
30. Rosso I, Saracco G, Specchia V (2003) Korean J Chem Eng 20:222–229
31. Tsoncheva T et al (2013) Appl Catal A 453:1–12
32. Konsolakis M et al (2013) J Hazad Mater 261:512–521
33. Aranda A et al (2012) Appl Catal B 127:77–88
34. Yang Z et al (2014) RSC Adv 4:39394–39399
35. Lapina OB et al (1999) Catal Today 51:469–479
36. El Assal Z et al (2013) Top Cata 56:679–687
37. Genuino HC et al (2012) J Phys Chem C 116:12066–12078
38. Vu VH et al (2008) AIChE J 54:1585–1591
39. Wu Z et al (2015) Mater Res. Bulletin 70:567–572
40. Carabineiro SAC et al (2015) Catal Today 244:103–114
41. Kim SC et al (2014) Powder Technol 266:292–298
42. Soylu GSP et al (2010) Chem Eng J. (Amsterdam, Netherlands) 162:380–387
43. Palacio LA et al (2008) Catal Today 133–135:502–508
44. Morales MR et al (2008) Fuel 87:1177–1186
45. Palacio LA et al (2008) J Hazad Mater 153:628–634
46. Wachs IE et al (2003) Catal Today 78:13–24
47. Fleury P (1966) Seances Acad Sci Ser C 263(22):1375–1377
48. Dunn JP et al (1999) Today 51:301–318
49. Kawada T, Hinokuma S, Machida M (2015) Catal Today 242:268–273